Blue Luminescent 2-(2‘-Pyridyl)benzimidazole Derivative Ligands and Their Orange Luminescent Mononuclear and Polynuclear Organoplatinum(II) Complexes

ARTICLE *in* INORGANIC CHEMISTRY · APRIL 2005

Impact Factor: 4.76 · DOI: 10.1021/ic0487530 · Source: PubMed

3 AUTHORS, INCLUDING:

Qinde Liu
Health Sciences Authority
39 PUBLICATIONS **1,195** CITATIONS

SEE PROFILE

Inorg. Chem. **2005**, *44*, 1332–1343

Blue Luminescent 2-(2′-Pyridyl)benzimidazole Derivative Ligands and Their Orange Luminescent Mononuclear and Polynuclear Organoplatinum(II) Complexes

Qin-De Liu, Wen-Li Jia, and Suning Wang*

Department of Chemistry, Queen's University, Kingston, Ontario K7L 3N6, Canada

Received September 6, 2004

Five new 2-(2′-pyridyl)benzimidazole derivative ligands, 1,4-bis[2-(2′-pyridyl)benzimidazolyl]benzene (1,4-bmb), 4,4′-bis[2-(2′-pyridyl)benzimidazolyl]biphenyl (bmbp), 1-bromo-4-[2-(2′-pyridyl)benzimidazolyl]benzene (Brmb), 1,3-bis-[2-(2′-pyridyl)benzimidazolyl]benzene (1,3-bmb), and 1,3,5-tris[2-(2′-pyridyl)benzimidazolyl]benzene (tmb), have been synthesized by Ullmann condensation methods. The corresponding mononuclear and polynuclear Pt^{II} complexes, Pt_2(1,4-bmb)Ph_4 (**1**), Pt_2(bmbp)Ph_4 (**2**), Pt(Brmb)Ph_2 (**3**), Pt_2(1,3-bmb)Ph_4 (**4**), and Pt_3(tmb)Ph_6 (**5**), have been obtained by the reaction of the appropriate ligand with $[PtPh_2(SMe_2)]_n$. The structures of the free ligands 1,4-bmb, bmbp, and tmb, as well as the complexes **1**–**3**, were determined by single-crystal X-ray diffraction. All ligands display fluorescent emissions in the purple/blue region of the spectrum at ambient temperature and phosphorescent emissions in the blue/green region at 77 K, which are attributable to ligand-centered $\pi \rightarrow \pi^*$ transition. No ligand-based emission was observed for the Pt^{II} complexes **1**–**5**. All Pt^{II} complexes display orange/red emissions at 77 K in a frozen solution or in the solid state, attributable to metal-to-ligand charge transfers (MLCT). Variable-temperature ^{1}H NMR experiments establish that complexes **1**, **4**, and **5** exist in isomeric forms in solution at ambient temperature due to the hindered rotation of the square PtC_2N_2 planes in the complexes.

Introduction

Since Tang and VanSlyke developed the first multilayer thin film devices based on tris(8-hydroxy quinolinato)-aluminum,[1] there has been much research effort on the investigation of new luminescent organic/organometallic compounds for use in the improvement of organic light-emitting devices (OLEDs).[2−6] It has been demonstrated that one of the key factors to obtain a stable OLED is the good film-forming capability of the deposited layers.[7] Starburst and long linear-shaped organic compounds with large conjugation systems have been found to often possess relatively high glass transition temperature (T_g) and very good film-forming properties.[8] Most of previously reported starburst molecules are based on 2,2′-diphenylamine or carbazole derivatives[9] due to the excellent hole transport properties of 2,2′-diphenylamino and carbazolyl units. Recent investigations on phosphorescent emitters for OLEDs have generated much interest in emitter materials containing heavy-metal centers.[3] Pt^{II} and Ir^{III} are among the most widely investigated

* Author to whom correspondence should be addressed. E-mail: wangs@chem.queensu.ca.

(1) Tang, C. W.; VanSlyke, S. A. *Appl. Phys. Lett.* **1987**, *51*, 913.
(2) (a) Tang, C. W.; VanSlyke, S. A.; Chen, C. H. *J. Appl. Phys.* **1989**, *65*, 3611. (b) Shirota, Y.; Kawami, S.; Imai, K. *Appl. Phys. Lett*. **1994**, *65*, 807. (c) Hamada, Y.; Sana, T.; Fujita, M.; Fujii, T.; Nishio, Y.; Shibata, K. *Jpn. J. Appl. Phys.* **1993**, *32*, L514. (d) Bulovic, V.; Gu, G.; Burrows, P. E.; Forrest, S. R. *Nature* **1996**, *380*, 29. (e) Braun, M.; Gmeiner, J.; Tzolov, M.; Coelle, M.; Meyer, F. D.; Milius, W.; Hillebrecht, H.; Wendland, O.; von Schutz, J. U.; Brutting, W. *J. Chem. Phys*. **2001**, *114*, 9625. (f) Schmidaur, H.; Lettenbauer, J.; Wikinson, D. L.; Müller, G.; Kumberger, O. *Z. Naturforsch*. **1991**, *46b*, 901.
(3) (a) Shen, Z.; Burrows, P. E.; Bulovic, V.; Borrest, S. R.; Thompson, M. E. *Science* **1997**, *276*, 2009. (b) Baldo, M. A.; Lamansky, S.; Burrows, P.; Thompson, M. E.; Forrest, S. R. *Appl. Phys. Lett*. **1999**, *75*, 5. (c) Kwong, R. C.; Sibley, S.; Dubovoy, T.; Baldo, M.; Forrest, S. R.; Thompson, M. E. *Chem. Mater*. **1999**, *11*, 3709 (d) Adachi, C.; Baldo, M. A.; Forrest, S. R.; Thompson, M. E. *Appl. Phys. Lett*. **2000**, *77*, 904. (e) Lamansky, S.; Djurovich, P.; Murphy, D.; Abdel-Razzaq, F.; Lee, H. E.; Adachi, C.; Burrows, P. E.; Forrest, S. R.; Thompson, M. E. *J. Am. Chem. Soc*. **2001**, *123*, 4304. (f) Liu, Q. D.; Thorne, L.; Kozin, I.; Song, D.; Seward, C.; D'Iorio, M.; Tao, Y.; Wang, S. *J. Chem. Soc., Dalton Trans*. **2002**, 3234. (g) Lu, W.; Mi, B. X., Chan, M. C. W.; Hui, Z.; Zhu, N.; Lee, S. T.; Che, C. M. *Chem. Commun.* **2002**, 206.
(4) (a) Li, Y.; Liu, Y.; Bu, W.; Guo, J.; Wang, Y. *Chem. Commun*. **2000**, 1551. (b) Popovic, Z. D.; Aziz, H.; Hu, N.-X.; Ioannidis, A.; dos Anjos, P. N. M. *J. Appl. Phys*. **2001**, *89*, 4673.(c) Adachi, C.; Tokito, S.; Tsutsui, T.; Saito, S. Jpn. *J. Appl. Phys*. **1988**, *27*, L713. (e) Tao, X. T.; Suzuki, H.; Wada, T.; Sasabe, H.; Miyata, S. *Appl. Phys. Lett*. **1999**, *75*, 1655. (f) Aziz, H.; Popovic, Z. D.; Hu, N.-X.; Hor, A.-M.; Xu, G. *Science* **1999**, *283*, 1900.

10.1021/ic0487530 CCC: $30.25
Published on Web 01/26/2005

metal centers because heavy metal centers with d^8 or d^6 electronic configurations can either enhance ligand-centered phosphorescent emission[3] or produce metal-to-ligand charge-transfer (MLCT) emission. As part of our research efforts to investigate the coordination chemistry of starburst organic compounds and develop new phosphorescent metal complexes, we reported recently a series of linear and starburst 2,2′-dipyridylamine derivative ligands[10] and the luminescent properties of their Pt^{II} complexes.[11] Although the free ligands based on 2,2′-dipyridylamine derivatives were demonstrated to be useful blue emitters in OLEDs,[10b] their Pt^{II} complexes were found to only display weak green phosphorescent emission at 77 K. The lack of phosphorescence by the Pt^{II} complexes at ambient temperature could be caused by the low rigidity of the six-membered chelate ring of the 2,2′-dipyridylamio group, which leads to the loss of energy by thermal vibrational decay.[12] To enhance the rigidity of the chelate, we synthesized a series of 2-(2′-pyridyl)benzimidazole derivative ligands. Similar to 2,2′-dipyridylamine, 2-(2′-pyridyl)benzimidazole also possesses two neutral nitrogen donors that can chelate to a metal center and an NH site that can be coupled to a carbon atom of different aryl groups, forming various interesting ligands. In contrast to the 2,2′-dipyridylamino group, the 2-(2′-pyridyl)benzimidazolyl group forms a five-membered chelate ring with a metal center, thus resulting in a relatively rigid chelate complex. In addition, the 2-(2′-pyridyl)benzimidazolyl group is more conjugated than 2,2′-dipyridylamino, which may result in a relatively low energy emission that is red-shifted, compared to that of the corresponding 2,2′-dipyridylamino complexes. Herein we report the results of our investigation on the new 2-(2′-pyridyl)benzimdazole derivative ligands and their corresponding Pt^{II} complexes.

Experimental Section

All starting materials were purchased from Aldrich Chemical Co. and used without further purification. All solvents used in syntheses and spectroscopic measurements were distilled over appropriate drying reagents. ^{1}H NMR and ^{13}C NMR were recorded on a Bruker Advance 500 MHz spectrometer operated at 500 MHz for ^{1}H and 125 MHz for ^{13}C. Excitation and emission spectra were obtained with a Photon Technologies International QuantaMaster model C-60 spectrometer. Emission lifetime was measured on a Photon Technologies International phosphorescent lifetime spectrometer, Timemaster C-631F equipped with a xenon flash lamp, and digital emission photon multiplier tube using a band pathway of 5 nm for excitation and 2 nm for emission. UV−vis spectra were recorded on a Hewlett-Packard 8452A diode array spectrophotometer. Cyclic voltammetry was performed using a BAS CV-50W analyzer with scan rates of 100 mV s^{-1}. The electrolytic cell used was a conventional three-compartment cell, in which a Pt working electrode, a Pt auxiliary electrode, and Ag/AgCl reference electrode were employed. The CV measurements were performed at room temperature using 0.10 M tetrabutylammonium hexafluorophosphate (TBAP) as the supporting electrolyte. The ferrocenium/ferrocene couple was used as the internal standard. Elemental analyses were performed by Canadian Microanalytical Service Ltd., Delta, British Columbia, Canada. The syntheses of the ligands 1,4-bmb, bmbp, Brmb, 1,3-bmb, and tmb were achieved by a modified Ullmann condensation method reported previously.[13] The Pt^{II} starting material $[PtPh_2(SMe_2)]_n$ ($n = 2$ or 3) was prepared using a procedure reported in the literature.[14]

Syntheses of 1,4-Bis[2-(2′-pyridyl)benzimidazolyl]bezene (1,4-bmb) and 1-Bromo-4-[2-(2′-pyridyl)benzimidazolyl]benzene (Brmb). A mixture of 1,4-dibromobenzene (0.50 g, 2.12 mmol), 2-(2′-pyridyl)benzimidazole (0.99 g, 5.0 mmol), CuI (0.081 g, 0.43 mmol), 1,10-phenanthroline (0.16 g, 0.88 mmol), and Cs_2CO_3 (2.9 g, 8.9 mmol) was suspended in 3.0 mL of DMF. The mixture was refluxed for 24 h and then cooled to room temperature. The resulting brown sticky residue was extracted with CH_2Cl_2 (50 mL × 4), and the organic extracts were combined, dried over $MgSO_4$, and purified by column chromatography (1:1 THF/hexane) to obtain the crude product of 1,4-bmb as light yellow powder. Recrystallization of the crude product in $CHCl_3$/hexanes afforded 1,4-bmb as colorless crystals (0.40 g, 35%). Mp: 229−230 °C. ^{1}H NMR (CD_2Cl_2, δ, ppm): 8.46 (d, 2H, $J = 4.7$ Hz, py), 8.31 (d, 2H, $J = 7.9$ Hz, py), 7.91 (dd, 2H, $J = 6.5$, 1.8 Hz, benzimidazolyl), 7.88 (td, 2H, $J = 7.8$, 1.7 Hz, py), 7.48 (s, 4H, Ph), 7.37−7.44 (m, 6H, benzimidazolyl), 7.35 (ddd, 2H, $J = 7.5$, 4.8, 1.0 Hz, py). ^{13}C NMR (CD_2Cl_2, δ, ppm): 151.0, 149.9, 149.0, 143.3, 138.2, 138.0, 137.0, 128.6, 125.0, 124.3, 124.2, 123.5, 120.5, 111.2. Anal. Calcd for $C_{30}H_{20}N_6$: C, 77.57; H, 4.31; N, 18.10. Found: C, 77.83; H, 4.14; N, 18.20. Column chromatography also gave rise to the monosubstituted product, Brmb, which was further purified by recrystallization in $CHCl_3$/hexanes (0.24 g, 32%). Mp: 168−170 °C. ^{1}H NMR (CD_2Cl_2, δ, ppm): 8.37 (d, 1H, $J = 4.6$ Hz, py), 8.28 (d, 1H, $J = 7.9$ Hz, py), 7.87 (d, 1H, $J = 8.0$ Hz, benzimidazolyl), 7.84 (td, 1H, $J = 7.8$, 1.8 Hz, py), 7.66 (d, 2H, $J = 8.7$ Hz, Ph), 7.38 (td,

(5) (a) Hamada, Y.; Sana, T.; Fujii, T.; Nishio, Y.; Takahashi, H.; Shibata, K. *Appl. Phys. Lett.* **1997**, *71*, 3338. (b) Hamada, Y.; Sano, T.; Fujita, M.; Fujii, T.; Nishio, Y.; Shibata, K. *Chem. Lett.* **1993**, 905.

(6) (a) Wu. Q.; Esteghamatian, M.; Hu, N.-X.; Popovic, Z.; Enright, G.; Tao, Y.; D'Iorio, M.; Wang, S. *Chem. Mater.* **2000**, *12*, 79. (b) Liu, Q. D.; M. S. Mudadu; H. Schmider; R. Thummel; Y. Tao; S. Wang. *Organometallics* **2002**, *21*, 4743. (c) Jia, W. L.; Bai, D. R.; McCormick, T.; Liu, Q. D.; Motala, M.; Wang, R. Y.; Seward, C.; Tao, Y.; Wang S. *Chem.*−*Eur. J.* **2004**, *10*, 994. (d) Lee, J.; Liu, Q. D.; Kang, Y.; Wang, S. *Chem. Mater.* **2004**, *16*, 1869. (e) Hu, N.-X.; Esteghamatian, M.; Xie, S.; Popovic, P.; Ong, B.; Hor, A.-M.; Wang, S. *Adv. Mater.* **1999**, *11*, 1460.

(7) Adachi, C.; Tsutsui, T.; Saito, S. *Appl. Phys. Lett.* **1990**, *56*, 799.

(8) Shirota, Y. *J. Mater. Chem.* **2000**, *10*, 1 and references therein.

(9) (a) Utsumi, H.; Nagahama, D.; Nakano, H.; Shirota, Y. *J. Mater. Chem.* **2002**, *12*, 2612. (b) Ogawa, H.; Ohnishi, K.; Shirota, Y. *Synth. Met.* **1997**, *91*, 243. (c) Utsumi, H.; Nagahama, D.; Nakano, H.; Shirota, Y. *J. Mater. Chem.* **2000**, *10*, 2436. (d) Noda, T.; Ogawa, H.; Noma, N.; Shirota, Y. *J. Mater. Chem.* **1999**, *9*, 2177. (e) Shirota, Y.; Moriwaki, K.; Yoshikawa, S.; Ujike, T.; Nakano, H. **1998**, *8*, 2579. (f) Ogawa, H.; Shirota, Y. *Appl. Phys. A* **1998**, *67*, 599. (g) Shirota, Y.; Okumoto, K.; Inada, H. *Synth. Met.* **2000**, *111*−*112*, 387. (h) Itano, K.; Tsuzuki, T.; Ogawa, H.; Appleyard, S.; Willis, M. R.; Shirota, Y. *IEEE Trans. Electron Devices* **1997**, *44*, 1218. (i) Ogawa, H.; Ohnishi, K.; Shirota, Y. *Synth. Met.* **1997**, *91*, 243. (j) Elschner, A.; Bruder, F.; Heuer, H. W.; Jonas, F.; Karbach, A.; Kirchmeyer, S.; Thurm, S.; Wehrmann, R. *Synth. Met.* **2000**, *111*−*112*, 139.

(10) (a) Yang, W. Y.; Chen, L.; Wang, S. *Inorg. Chem.* **2001**, *40*, 507. (b) Pang, J.; Tao, Y.; Freiberg, S.; Yang, X. P.; D'Iorio, M.; Wang, S. *J. Mater. Chem.* **2002**, *12*, 206.

(11) Liu Q. D.; Jia, W. L.; Wu, G.; Wang, S. *Organometallics* **2003**, *22*, 3781.

(12) (a) Lakowicz, J. R. *Principle of Fluorescence Spectroscopy*, 2nd ed.; Kluwer Academic: New York, 1999. (b) Ingle, J. D., Jr.; Crouch, S. R. *Spectrochemical Analysis*; Prentice Hall: Englewood Cliffs, NJ, 1988; Chapter 12.

(13) Klapars, A.; Antilla, J. C.; Huang, X. H.; Buchwald, S. L. *J. Am. Chem. Soc.* **2001**, *123*, 7727.

(14) (a) Hill, G. S.; Irwin, M. J.; Levy, C. J.; Rendina, L. M.; Puddephatt, R. J. *Inorg. Synth.* **1998**, *32*, 149. (b) Song, D.; Wang, S. *J. Organomet. Chem.* **2002**, *648*, 302.

1H, J = 7.5, 1.2 Hz, benzimidazolyl), 7.34 (td, 1H, J = 8.0, 1.2 Hz, benzimidazolyl), 7.29 (ddd, 1H, J = 7.5, 4.8, 1.0 Hz, py), 7.24−7.27 (m, 3H, Ph and benzimidazolyl). ^{13}C NMR (CD_2Cl_2, δ, ppm): 150.8, 149.8, 149.0, 143.3, 138.1, 137.6, 137.0, 132.7, 129.6, 124.9, 124.3, 124.2, 123.5, 120.4, 111.1, 110.2. HRMS: calcd for M^+ ($C_{18}H_{11}N_3Br$), m/z 348.0136; found, m/z 348.0131.

Synthesis of 4,4′-Bis[2-(2′-pyridyl)benzimidazolyl]biphenyl (bmbp). Bmbp was synthesized in the same manner as described for 1,4-bmb. In the presence of CuI (0.049 g, 0.26 mmol), 1,10-phenanthroline (0.095 g, 0.63 mmol), and Cs_2CO_3 (1.75 g, 5.4 mmol), the reaction of 4,4′-diiodobiphenyl (0.52 g, 1.29 mmol) with 2-(2′-pyridyl)benzimidazole (0.60 g, 3.0 mmol) afforded bmbp as colorless crystals (0.47 g, 68%). Mp: >300 °C. ^{1}H NMR (CD_2Cl_2, δ, ppm): 8.45 (d, 2H, J = 5.0 Hz, py), 8.22 (d, 2H, J = 7.8 Hz, py), 7.97 (d, 2H, J = 8.0 Hz, benzimidazolyl), 7.80−7.83 (m, 6H, Ph and py), 7.47 (d, 4H, J = 8.3 Hz, ph), 7.41 (ddd, J = 8.1, 5.7, 2.5 Hz, benzimidazolyl), 7.33−7.37 (m, 4H, benzimidazolyl), 7.27 (dd, 2H, J = 7.5, 5.5 Hz, py). ^{13}C NMR (CD_2Cl_2, δ, ppm): 150.9, 149.8, 149.4, 143.1, 140.2, 138.0, 137.7, 136.9, 128.3, 128.2, 125.1, 124.5, 124.2, 123.7, 120.7, 111.3. Anal. Calcd for $C_{36}H_{24}N_6$·0.1$CHCl_3$: C, 78.47; H, 4.40; N, 15.21. Found: C, 78.64; H, 4.46; N, 15.11.

Syntheses of 1,3,5-Tris[2-(2′-pyridyl)benzimidazolyl]benzene (tmb) and 1,3-Bis[2-(2′-pyridyl)benzimidazolyl]benzene (1,3-bmb). Tmb and 1,3-bmb were obtained in the same manner as described for 1,4-bmb except that reaction was kept refluxing for 72 h instead of 24 h. In the presence of CuI (0.11 g, 0.58 mmol), 1,10-phenantholine (0.21 g, 1.17 mmol), and Cs_2CO_3 (4.13 g, 12.7 mmol), the reaction of 1,3,5-tribromobenzene (0.60 g, 1.9 mmol) with 2-(2′-pyridyl)indolyl (1.3 g, 6.7 mmol) afforded tmb and 1,3-bmb. These two compounds were separated by column chromatograph using THF/hexane/MeOH (1:1:0.05) as the eluent, and the crude products were recrystallized from CH_2Cl_2/hexanes to afford tmb (0.50 g, 40%) and 1,3-bmb (0.28 g, 32%) as colorless crystals. Tmb: mp 277−279 °C; ^{1}H NMR (CD_2Cl_2, δ, ppm) 8.49 (d, 3H, J = 4.5 Hz, py), 8.30 (d, 3H, J = 7.9 Hz, py), 7.90 (d, 3H, J = 8.0 Hz, benzimidazolyl), 7.83 (t, 3H, J = 7.7 Hz, py), 7.51 (s, 3H, Ph), 7.37 (t, 3H, J = 8.1 Hz, benzimidazolyl), 7.33 (dd, 3H, J = 8.0, 4.9 Hz, py), 7.29 (t, 3H, J = 7.9 Hz, benzimidazolyl), 7.21 (d, 3H, J = 8.1, benzimidazolyl); ^{13}C NMR (CD_2Cl_2, δ, ppm) 150.6, 149.7, 149.1, 143.1, 139.7, 138.0, 137.2, 127.1, 125.1, 124.6, 124.4, 123.9, 120.8, 110.9. Anal. Calcd for $C_{42}H_{27}N_9$·0.25CH_2Cl_2: C, 74.74; H, 4.08; N, 18.57. Found: C, 74.68; H, 4.55; N, 18.43. 1,3-bmb: mp 190−192 °C; ^{1}H NMR 8.43 (d, 2H, J = 5.8 Hz, py), 8.27 (d, 2H, J = 7.9 Hz, py), 7.87 (d, 2H, J = 8.1 Hz, benzimidazolyl), 7.85 (t, 2H, J = 7.8 Hz, py), 7.65 (t, 1H, J = 7.9 Hz, Ph), 7.48 (d, 2H, J = 7.9 Hz, Ph), 7.30−7.39 (m, 7H, py, benzimidazolyl, ph), 7.25 (d, 2H, J = 7.9 Hz, benzimidazolyl); ^{13}C NMR (CD_2Cl_2, δ, ppm) 150.8, 149.9, 149.0, 143.2, 139.2, 138.2, 137.6, 137.0, 130.9, 127.5, 125.0, 124.3, 124.2, 120.4, 111.1; HRMS calcd for $(M - H)^+$ ($C_{30}H_{20}N_6$) m/z 464.174 9, found m/z 464.172 9.

Synthesis of Pt_2(1,4-bmb)Ph_4 (1). A mixture of 1,4-bmb ligand (30 mg, 0.064 mmol) and $[PtPh_2(SMe_2)]_n$ (53 mg, 0.129 mmol Pt) was dissolved in 10 mL of CH_2Cl_2. Then 5 mL of hexane was successfully layered upon the solution. Slow evaporation of the solvent and diffusion of hexane into the CH_2Cl_2 layer afforded complex **1** as orange crystals after 2 days (68 mg, 91% yield). ^{1}H NMR (DMSO-d_6, δ, ppm): 8.38 (d, 1H, J = 4.7 Hz, py), 8.36 (d, 1H, J = 4.5 Hz, py), 8.28 (s, 2H, central Ph), 8.27 (s, 2H, central Ph), 8.26 (t, 1H, J = 8.1 Hz, py), 8.20 (t, 1H, J = 8.2 Hz, py), 7.67 (m, 2H, py), 7.58 (d, 4H, J = 6.7 Hz, Ph), 7.39−7.48 (m, 9H, Ph, benzimidazolyl, and Py), 7.20 (d, 1H, J = 8.3 Hz, py), 7.13 (t, 1H, J = 6.7 Hz, benzimidazolyl), 7.10 (t, 1H, J = 7.1 Hz, benzimidazolyl), 6.93 (t, 4H, J = 7.2 Hz, Ph), 6.91 (t, 4H, J = 6.8 Hz, Ph), 6.83 (t, 2H, J = 7.2 Hz, Ph), 6.78 (t, 2H, J = 7.1 Hz, Ph), 6.50 (d, 1H, J = 8.0 Hz, benzimidazolyl), 6.48 (d, 1H, J = 8.0 Hz, benzimidazolyl). The ^{13}C NMR spectrum could not be obtained due to poor solubility. Anal. Calcd for $C_{54}H_{40}N_6Pt_2$: C, 55.77; H, 3.47; N, 7.23. Found: C, 55.89; H, 3.48; N, 7.12.

Synthesis of Pt_2(bmbp)Ph_4 (2). In the same manner as described for **1** except layering toluene instead of hexane upon the solution, the reaction of bmbp (50 mg, 0.093 mmol) and $[PtPh_2(SMe_2)]_n$ (76 mg, 0.185 mmol Pt) afforded complex **2** as orange crystals (103 mg, 89% yield). ^{1}H NMR (DMSO-d_6, δ, ppm): 8.33 (m, 6H, py and central Ph), 8.09 (t, 2H, J = 7.7 Hz, py), 8.02 (d, 2H, J = 8.1 Hz, central Ph), 7.61 (t, 2H, J = 7.5 Hz, py), 7.58 (d, 4H, J = 7.3 Hz, Ph), 7.47 (d, 4H, J = 7.0 Hz, Ph), 7.36 (t, 2H, J = 8.0 Hz, benzimidazolyl), 7.18 (d, 2H, J = 8.2 Hz, benzimidazolyl), 7.13 (d, 2H, J = 8.0 Hz, py), 7.09 (t, 2H, J = 7.5 Hz, benzimidazolyl), 6.93 (t, 4H, J = 7.5 Hz, Ph), 6.91 (t, 4H, J = 7.5 Hz, Ph), 6.83 (t, 2H, J = 7.4 Hz, Ph), 6.77 (t, 2H, J = 7.2 Hz, Ph), 6.48 (d, 2H, J = 8.2 Hz, benzimidazolyl). The ^{13}C NMR spectrum could not be obtained due to poor solubility. Anal. Calcd for $C_{60}H_{44}N_6Pt$·CH_2Cl_2: C, 55.33; H, 3.47; N, 7.23. Found: C, 54.85; H, 3.48; N, 7.12.

Synthesis of Pt(Brmb)Ph_2 (3). In the same manner as described for **1** except layering toluene instead of hexane upon the solution, the reaction of Brmb (20 mg, 0.057 mmol) and $[PtPh_2(SMe_2)]_n$ (25 mg, 0.060 mmol Pt) afforded complex **3** as orange crystals (35 mg, 88% yield). ^{1}H NMR (DMSO-d_6, δ, ppm): 8.31 (d, 1H, J = 5.0 Hz, py), 8.09 (d, 1H, J = 8.0 Hz, py), 8.01 (d, 2H, J = 8.6 Hz, Ph−Br), 7.81 (d, 2H, J = 8.6 Hz, Ph−Br), 7.59 (dd, 1H, J = 7.5, 5.4 Hz, py), 7.55 (d, 2H, J = 7.5 Hz, Ph), 7.45 (d, 2H, J = 7.8 Hz, Ph), 7.31 (t, 1H, J = 8.2 Hz, benzimidazolyl), 7.12 (d, 1H, J = 8.4 Hz, benzimidazolyl), 7.05 (t, 1H, J = 8.2 Hz, benzimidazolyl), 7.02 (d, 1H, J = 8.1 Hz, py), 6.91 (t, 2H, J = 7.2 Hz, Ph), 6.90 (t, 2H, J = 7.4 Hz, Ph), 6.81 (t, 1H, J = 7.2 Hz, Ph), 6.76 (t, 1H, J = 7.3 Hz, Ph), 6.44 (d, 1H, J = 8.4 Hz, benzimidazolyl). The ^{13}C NMR spectrum could not be obtained due to poor solubility. Anal. Calcd for $C_{30}H_{22}N_3BrPt$·1.5C_7H_8: C, 58.06; H, 4.06; N, 5.02. Found: C, 57.93; H, 4.13; N, 4.73.

Synthesis of Pt_2(1,3-bmb)Ph_4 (4). In the same manner as described for **1** except layering toluene instead of hexane upon the solution, the reaction of 1,3-bmb (30 mg, 0.064 mmol) and $[PtPh_2(SMe_2)]_n$ (76 mg, 0.129 mmol Pt) afforded complex **4** as orange crystals (66 mg, 89% yield). ^{1}H NMR (DMSO-d_6, δ, ppm): 8.25−8.35 (m, 6H, py and central Ph), 8.19 (t, 1H, J = 8.0 Hz, py), 8.12 (t, 1H, J = 7.7 Hz, py), 7.62 (m, 2H, py), 7.53 (d, 4H, J = 7.0 Hz, Ph), 7.39−7.44 (m, 5H, Ph and py), 7.36 (d, 2H, J = 7.5 Hz, benzimidazolyl), 7.33 (t, 2H, J = 7.7 Hz, benzimidazolyl), 7.07 (t, 2H, J = 7.3 Hz, benzimidazolyl), 6.89 (m, 8H, Ph), 6.80 (t, 2H, J = 7.2 Hz, Ph), 6.76 (t, 2H, J = 7.3 Hz, Ph), 6.45 (d, 1H, J = 8.0 Hz, benzimidazolyl), 6.43 (d, 1H, J = 8.0 Hz, benzimidazolyl). The ^{13}C NMR spectrum could not be obtained due to poor solubility. Anal. Calcd for $C_{54}H_{40}N_6Pt_2$·0.25CH_2Cl_2·0.5C_7H_8: C, 56.38; H, 3.62; N, 6.83. Found: C, 56.30; H, 3.56; N, 6.76.

Synthesis of Pt_3(tmb)Ph_6 (5). In the same manner as described for **1** except layering toluene instead of hexane upon the solution, the reaction of tbp (50 mg, 0.076 mmol) and $[PtPh_2(SMe_2)]_n$ (95 mg, 0.23 mmol Pt) afforded complex **5** as orange crystals (110 mg, 85% yield). ^{1}H NMR (DMSO-d_6, δ, ppm, 298 K): 8.96 (s, 2H), 8.85 (s, 1H), 8.30−8.37 (m, 4H), 8.14 (t, 2H, J = 8.0 Hz), 7.35−7.82 (m, 24 H), 7.07−7.13 (m, 3H), 6.88−6.91 (m, 12H), 6.74−6.82 (m, 6H), 6.47 (d, 1H, J = 8.2 Hz), 6.43 (d, 2H, J = 8.2 Hz). The ^{13}C NMR spectrum could not be obtained due to poor

Table 1. Crystal Data for 1,4-bmb, bmbp, tmb, and Complexes **1**−**3**

	1,4-bmb	bmbp	tmb	1	2	3
formula	$C_{30}H_{20}N_6 \cdot 2CHCl_3$	$C_{36}H_{24}N_6 \cdot 2CHCl_3$	$C_{42}H_{27}N_9 \cdot 1.5CH_2Cl_2$	$C_{54}H_{40}N_6Pt_2 \cdot 2CH_2Cl_2 \cdot$ 2hexane	$C_{60}H_{44}N_6Pt_2 \cdot 2CH_2Cl_2$	$C_{30}H_{22}N_3BrPt \cdot 2C_7H_8$
fw	703.26	779.35	785.11	1505.30	1409.04	833.77
cryst system	monoclinic	monoclinic	monoclinic	monoclinic	triclinic	monoclinic
space group	$P2_1/c$	$P2_1/c$	$I2/a$	$P2_1/n$	$P\bar{1}$	$P2_1/c$
a/Å	9.4513(18)	6.158(3)	22.002(5)	12.571(3)	9.6917(15)	10.348(3)
b/Å	20.766(4)	32.742(18)	13.385(3)	18.355(4)	11.5099(18)	19.768(6)
c/Å	8.6353(16)	9.152(5)	27.273(7)	13.389(3)	13.659(2)	18.316(5)
α/deg	90	90	90	90	91.300(2)	90
β/deg	110.685(3)	96.325(12)	90.178(6)	91.310(4)	106.758(2)	93.892(5)
γ/deg	90	90	90	90	108.803(2)	90
V/Å^3	1585.5(5)	1834.0(17)	8032(3)	3088.6(13)	1369.9(4)	3738.0(18)
Z	2	2	8	2	1	4
D_c/g cm^{-3}	1.473	1.411	1.299	1.619	1.708	1.570
μ/mm^{-1}	0.576	0.506	0.272	4.744	5.342	4.857
$2\theta_{max}$/deg	56.60	56.66	56.60	56.62	56.58	56.68
no. of rflcns measd	11 445	12 318	27 981	19 713	9900	26 434
no. of rflcns used	3810	4190	9254	7275	6271	8753
R_{int}	0.0345	0.0664	0.0375	0.0663	0.0138	0.1997
no. of params	230	226	545	358	352	394
final R [$I > 2\sigma(I)$]						
R1[a]	0.0394	0.0719	0.0686	0.0572	0.0761	0.0822
wR2[b]	0.0756	0.1544	0.1878	0.1167	0.2053	0.1611
R (all data)						
R1[a]	0.1281	0.2415	0.1442	0.1788	0.0912	0.2913
wR2[b]	0.0900	0.2097	0.2225	0.1436	0.2184	0.2019
goodness of fit on F^2	0.757	0.793	0.923	0.810	1.053	0.748

[a] $R1 = \sum[|F_o| - |F_c|]/\sum|F_o|$. [b] $wR2 = \{\sum[w(F_o^2 - F_c^2)]/\sum(wF_o^2)\}^{1/2}$. $w = 1/[\sigma^2(F_o^2) + (0.075P)^2]$, where $P = [\max(F_o^2,0) + 2F_c^2]/3$.

solubility. Anal. Calcd for $C_{78}H_{57}N_9Pt_3 \cdot 1.5CH_2Cl_2 \cdot 2C_7H_8$: C, 55.67; H, 3.67; N, 6.25. Found: C, 55.44; H, 3.70; N, 6.11.

X-ray Crystallographic Analysis. Single crystals of 1,4-bmb, bmbp, and tmp ligands and the complexes **1**−**3** were obtained and characterized by X-ray diffraction analysis. Crystals were mounted on glass fibers for data collection. Data were collected on a Siemens P4 single-crystal X-ray diffractometer with a Smart CCD-1000 detector and graphite-monochromated Mo Kα radiation, operating at 50 kV and 35 mA at 25 °C. The data collection ranges of 2θ are 3.92−56.60° for 1,4-bmb, 4.64−56.66° for bmbp, 5.02−56.60° for tmb, 4.40−56.62° for complex **1**, 3.04−56.86° for complex **2**, and 3.14−56.58° for complex **3**. No significant decay was observed for all of the samples. Data were processed on a PC using the Bruker SHELXTL software package[15] (version 5.10) and were corrected for Lorentz and polarization effects. Ligands 1,4-bmb and bmbp and complex **3** crystallize in the monoclinic space group $P2_1/c$, and the molecules of 1,4-bmb and bmbp possess an inversion center. The crystals of tmp belong to the body-centered monoclinic space group $I2/a$. Complexes **1** and **2** crystallize in monoclinic space group $P2_1/n$ and triclinic space group $P\bar{1}$, respectively, and their molecules possess an inversion center. All non-hydrogen atoms except the solvent molecules and a few carbon atoms (C7 and C12) in complex **3** were refined anisotropically. Complex **3** crystallized as very thin needle crystals, which diffract poorly, greatly reducing the quality of its crystallographic data. As a result, one of the coordinated phenyl groups (C7−C12) in **3** had to be refined as a rigid body to obtain meaningful Pt−C bond distances. All hydrogen atoms except those of the disordered solvent molecules were calculated, and their contributions in structural factor calculations were included. The crystallographic data are given in Table 1. Selected bond lengths and angles for complexes **1**−**3** are listed in Table 2.

(15) *SHELXTL NT Crystal Structure Analysis Package*, version 5.10; Bruker Axs Analytical X-ray System: Madison, WI, 1999.

Table 2. Selected Bond Lengths (Å) and Angles (deg) for Complexes **1**−**3**

	Complex **1**		
Pt(1)−C(1)	2.019(13)	Pt(1)−C(7)	1.974(13)
Pt(1)−N(1)	2.156(8)	Pt(1)−N(2)	2.129(8)
C(1)−Pt(1)−C(7)	87.4(4)	C(1)−Pt(1)−N(1)	95.1(4)
C(1)−Pt(1)−N(2)	172.4(4)	C(7)−Pt(1)−N(1)	177.0(4)
C(7)−Pt(1)−N(2)	100.0(4)	N(1)−Pt(1)−N(2)	77.4 (3)
	Complex **2**		
Pt(1)−C(1)	1.974(13)	Pt(1)−C(7)	1.997(11)
Pt(1)−N(1)	2.130(10)	Pt(1)−N(2)	2.109(9)
C(1)−Pt(1)−C(7)	88.0(4)	C(1)−Pt(1)−N(1)	97.6(4)
C(1)−Pt(1)−N(2)	172.0(4)	C(7) − Pt(1)−N(1)	174.0(4)
C(7)−Pt(1)−N(2)	97.3(4)	N(1)−Pt(1)−N(2)	76.8(3)
	Complex **3**		
Pt(1)−C(1)	1.914(18)	Pt(1)−C(7)	1.950(9)
Pt(1)−N(1)	2.132(16)	Pt(1)−N(2)	2.088(15)
C(1)−Pt(1)−C(7)	87.2(6)	C(1)−Pt(1)−N(1)	96.8(6)
C(1)−Pt(1)−N(2)	171.5(7)	C(7)−Pt(1)−N(1)	175.9(5)
C(7)−Pt(1)−N(2)	99.6(6)	N(1)−Pt(1)−N(2)	76.3(7)

Results and Discussion

Syntheses. All new 2-(2′-pyridyl)benzimidazole derivative ligands were synthesized in good yield using the modified Ullmann condensation procedures depicted in Scheme 1, where an appropriate aryl halide reacts with 2-(2′-pyridyl)-benzimidazole in the presence of CuI catalyst, 1,10-phenathroline, and Cs_2CO_3. The size of the cation of the base does have an effect on the yield of the coupling reaction of the aryl halide and 2-(2′-pyridyl)benzimidazole,[13] as indicated by the much higher yield of the reaction using Cs_2CO_3 than K_2CO_3 (the latter only afforded trace product). The high reactivity of aryl iodide resulted in the isolation of the bisubstituted product bmbp from the reaction of 4,4′-diiodobiphenyl with benzimidazole in good yield (Scheme 1, top). In contrast, due to the relatively low reactivity of

Scheme 1

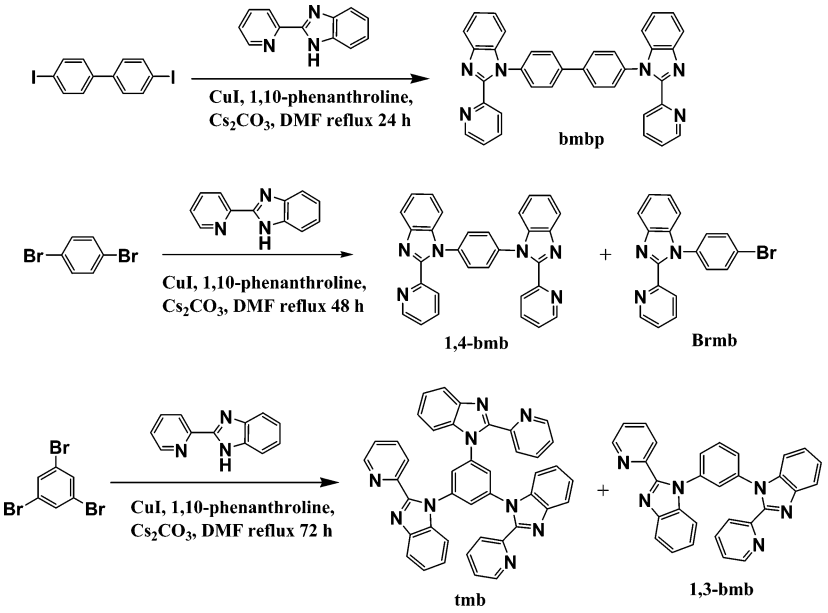

aryl bromide, the reaction of 1,4-dibromobenzene or 1,3,5-tribromobenzene with 2-(2′-pyridyl)benzimidazole gave rise to a mixture of two products (Scheme 1, middle and bottom), which can be separated by column chromatograph. For 1,4-dibromobenzene, the bisubstituted product bmb and the monosubstituted product BrmB were obtained. For 1,3,5-tribromobenzene, the trisubstituted product tmb and the bisubstituted product 1,3-bmb where a bromine atom was replaced by a hydrogen were isolated. Due to the steric effect, the reaction of 1,3,5-tribromobenzene with 2-(2′-pyridyl)-benzimidazole requires a long reaction time (reflux for 72 h) to produce the trisubstituted product. The bromine atom was probably lost due to thermal cleavage of the C−Br bond under the reaction conditions. All ligands are fully characterized by ^{1}H and ^{13}C NMR, elemental analyses, or high-resolution mass spectroscopy. Single-crystal X-ray diffraction analyses were performed for the 1,4-bmb, bmbp, and tmb ligands.

The Pt^{II} complexes **1**−**5** were synthesized by using $[PtPh_2(SMe_2)]_n$ as the starting material.[14] The reactions of $[PtPh_2(SMe_2)]_n$ with the corresponding ligand in a stoichiometric amount afforded the corresponding complexes in good yield. The relatively labile bridging ligand SMe_2 in $[PtPh_2(SMe_2)]_n$ was replaced by the chelating 2-(2′-pyridyl)-benzimidazolyl moiety in the resulting complexes. The synthetic routes for complexes **1**−**5** are summarized in Scheme 2. All complexes were characterized by ^{1}H NMR spectroscopy and elemental analyses. Due to their poor solubility in common organic solvents, ^{13}C NMR spectra for the complexes could not be obtained. The ^{1}H NMR spectra of complexes **1**, **4**, and **5** at ambient temperature are very complex, indicating either the presence of structural isomers or a slow exchange process. To establish the structures of the complexes, single-crystal X-ray analyses for complexes **1**−**3** were carried out. Many attempts were made to obtain

Scheme 2

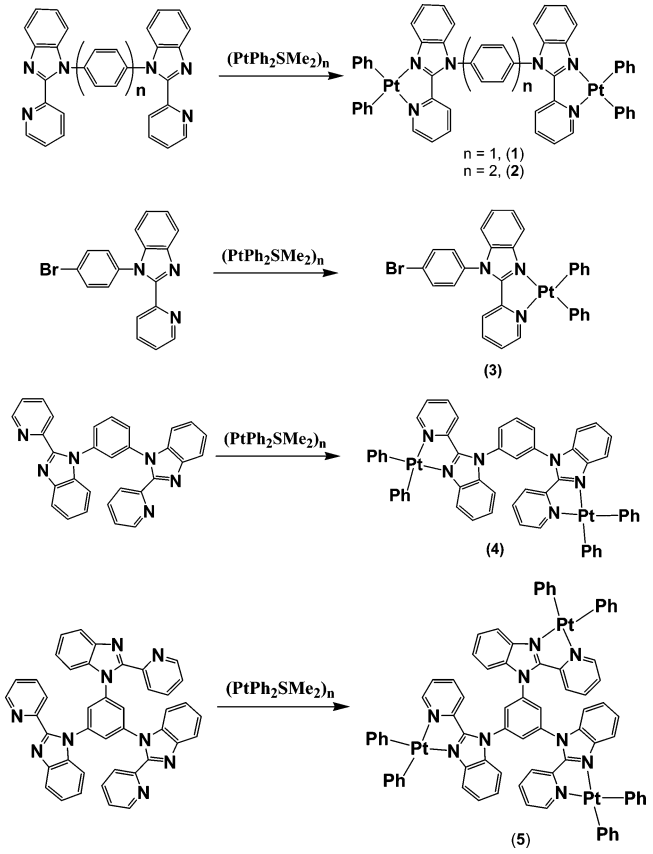

single-crystals of complexes **4** and **5** for X-ray diffraction. However, no suitable crystals for these two compounds were obtained.

Crystal Structures. Ligands. The crystal structure of 1,4-bmb is shown in Figure 1. The molecule of 1,4-bmb possesses an inversion center. The central phenyl ring is not coplanar with the benzimidazole ring, as indicated by the dihedral angle of 54.0° between the two planes. The pyridyl ring is also not coplanar with the benzimidazole ring, and

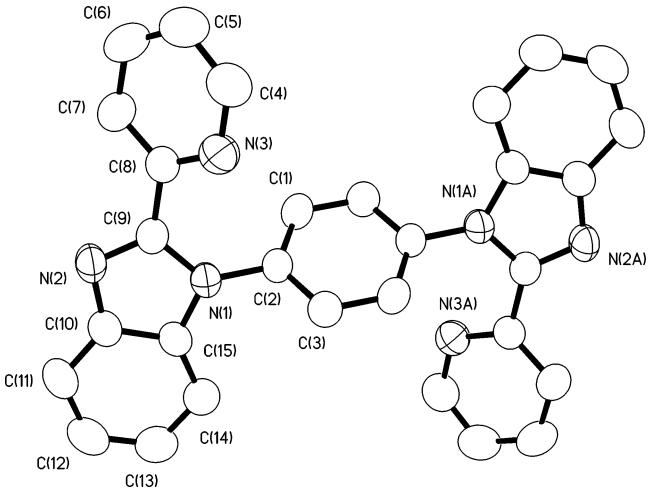

Figure 1. Molecular structure of bmb with 50% thermal ellipsoids and labeling schemes. All hydrogen atoms are omitted for clarity.

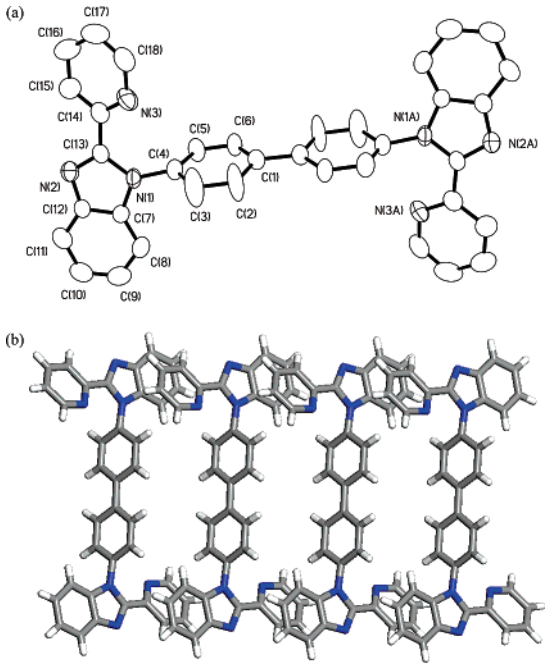

Figure 2. (a) Molecular structure of bmbp with 50% thermal ellipsoids and labeling schemes. All hydrogen atoms are omitted for clarity. (b) Ladderlike double chain structure formed by $\pi-\pi$ stacking in bmbp.

the dihedral angle between the two planes is 34.9°. Each benzimidazolyl group of 1,4-bmb has $\pi-\pi$ stacking with another benzimidazolyl group of an adjacent molecule, hence forming a 1D $\pi-\pi$ stacking chain structure (see Supporting Information). The distance between the stacked planes is 3.61 Å.

The crystal structure of bmbp is similar as that of 1,4-bmb as shown in Figure 2a. The molecule of bmbp also possesses an inversion center. The central biphenyl rings are coplanar. The benzimidazolyl ring is not coplanar with the biphenyl rings, as indicated by the dihedral angle of 69.2°. The pyridyl ring is almost coplanar with the benzimidazolyl ring, as shown by the dihedral angle of 15.1°. In the crystal lattice, each molecule of bmbp forms $\pi-\pi$ stacking with two neighboring molecules via the pyridyl and the benzimidazolyl rings, resulting in the formation of an interesting 1D

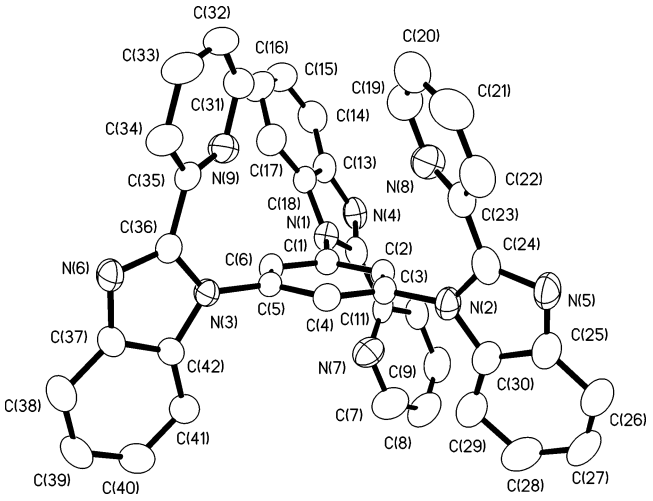

Figure 3. Molecular structure of tmb with 50% thermal ellipsoids and labeling schemes showing the cuplike structure of the molecule. All hydrogen atoms are omitted for clarity.

ladderlike structure as shown in Figure 2b. The distance between the stacked plane is about 3.57 Å.

The crystal structure of tmb is shown in Figure 3. The three pyridylbenzimidazolyl groups in tmb are almost perpendicular to the central phenyl ring, as indicated by the dihedral angles of 58.8, 73.1, and 86.6°, respectively. As a result, the molecule of tmb has a cuplike shape. As shown in Figure 3, two of the 2-(2′-pyridyl)benzimidazolyl groups are oriented to the same side of the central benzene ring while the third one is oriented to the opposite side of the benzene ring, perhaps to minimize steric interactions. If tmb retains the same structure in solution, the ^{1}H NMR spectrum of tmb should show two sets of chemical shifts of the 2-(2′-pyridyl)-benzimidazolyl. However, at ambient temperature, only one set of chemical shifts due to 2-(2′-pyridyl)benzimidazolyl was observed in the NMR spectrum of tmb, indicating that the three 2-(2′-pyridyl)benzimidazolyl groups have a symmetric arrangement in solution at ambient temperature. The molecules of tmb in the crystal lattice are paired up through $\pi-\pi$ stacking involving one of the 2-(2′-pyridyl)benzimidazolyl groups (see Supporting Information). The distance between the stacked planes is about 3.66 Å.

Complexes 1−3. The crystal structure of complex Pt_2(1,4-bmb)Ph_4 (**1**) is shown in Figure 4a. The molecule of complex **1** possesses an inversion center. Each Pt^{II} center in **1** is bidentately chelated by a 1,4-bmb ligand via the 2-(2′-pyridyl)benzimidazolyl unit and further coordinated by two phenyl ligands, forming a typical square-planar geometry. The square plane of the Pt center is somewhat distorted, as indicated by the bond angle of N(1)−Pt(1)−N(2) (77.4(3)°). The Pt−C and Pt−N bond lengths are typical for Pt^{II} complexes. The Pt center is coplanar with the 2-(2′-pyridyl)-benzimidazolyl plane. The structure of **1** supports that the environment around the Pt center in **1** has a much higher rigidity than that of the Pt^{II} complexes with the 2,2′-dipyridylamino derivative ligands, where the six-membered chelate ring is often not coplanar.[11] The PtC_2N_2 plane is almost perpendicular to the central benzene ring as indicated by the dihedral angle of ∼86.9°. The intramolecular Pt(1)−

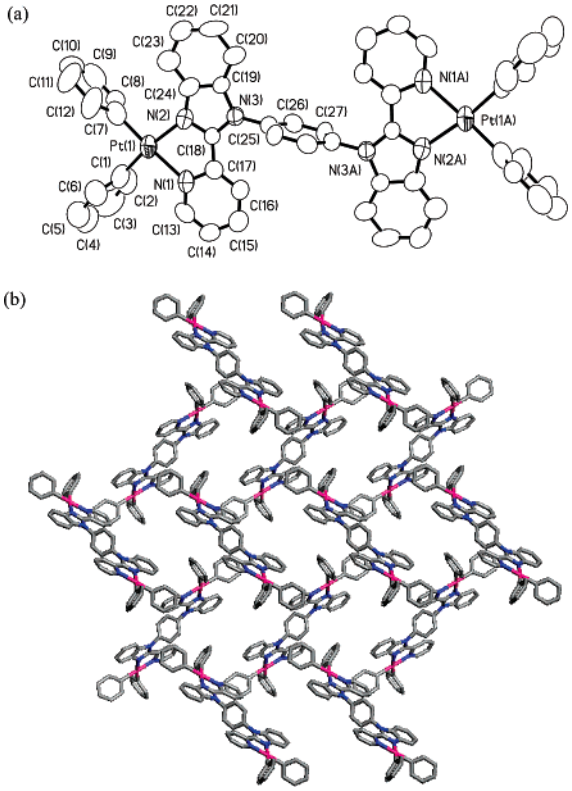

Figure 4. (a) Molecular structure of complex **1** with 50% thermal ellipsoids and labeling schemes. All hydrogen atoms are omitted for clarity. (b) Viewed along *a* axis, the packing diagram showing the honeycomb structure in complex **1**. Crystal solvent molecules are omitted for clarity.

Pt(1A) separation distance is 13.391(4) Å. The shortest intermolecular Pt−Pt distance is 9.093(4) Å. There is no significant $\pi-\pi$ stacking interaction. When viewed along *a* axis, an interesting honeycomb structure was observed for **1** (Figure 4b), which traps CH_2Cl_2 and hexane solvent molecules in the cavities.

The crystal structure of $Pt_2(bmbp)Ph_4$ (**2**) resembles that of **1** as shown in Figure 5a. The molecule of **2** also possesses an inversion center. The Pt center in **2** has a coordination environment similar to that in **1**. The central biphenyl unit is coplanar but is nearly perpendicular to the PtC_2N_2 plane (dihedral angle 84.5°). Due to the presence of the biphenyl group in **2**, the intramolecular Pt−Pt distance is very long (17.421(4) Å). The shortest Pt−Pt distance in **2** is intermolecular separation between Pt(1) and Pt(1′) (6.738(4) Å). Despite the similarity of the molecular structures of **1** and **2**, their extended structures are quite different. There is no $\pi-\pi$ stacking interaction in **1**. However, a $\pi-\pi$ stacked 1D chain structure was observed in crystal lattice of **2**. As shown in Figure 5b, the two 2-(2′-pyridyl)benzimidazolyl units of **2** form $\pi-\pi$ stacking with other two 2-(2′-pyridyl)benzimidazolyl units from two neighboring molecules, leading to the formation of a 1D chain structure. All the 1D chains are parallel with each other with the distance between the stacked plane being 3.69 Å.

The crystal structure of complex $Pt(Brmb)Ph_2$ (**3**) is shown in Figure 6. The environment around the Pt center in **3** resembles those of **1** and **2**. Complex **3** could be regarded as half of the molecule of **2**. Again the PtC_2N_2 plane is almost

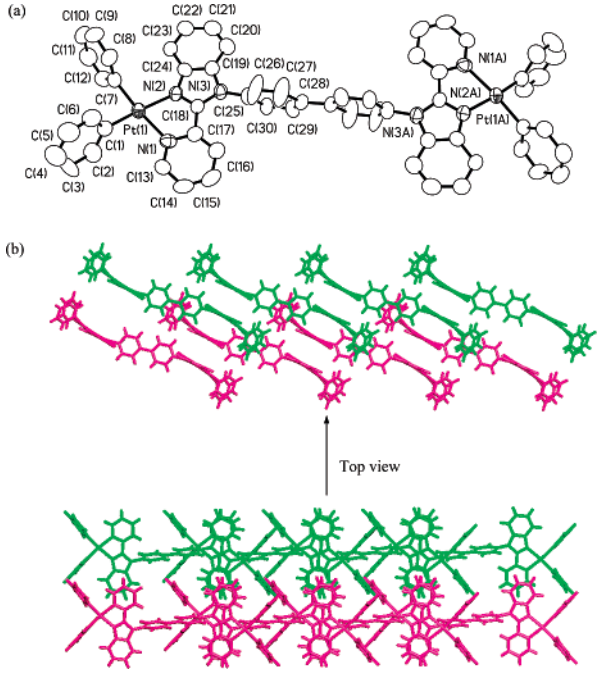

Figure 5. (a) Molecular structure of complex **2** with 50% thermal ellipsoids and labeling schemes. All hydrogen atoms are omitted for clarity. (b) Parallel 1D chain structure formed by intermolecular $\pi-\pi$ stacking in complex **2**.

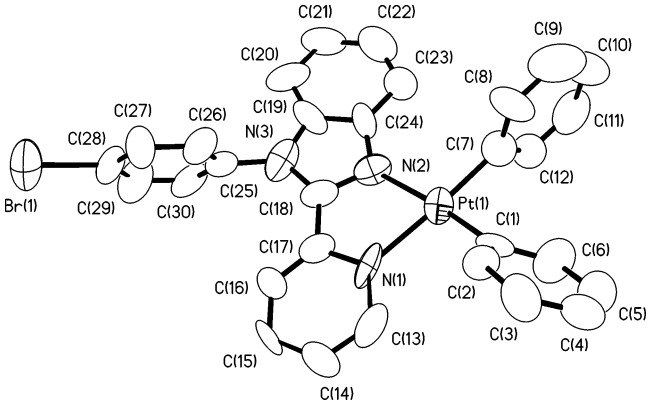

Figure 6. Molecular structure of complex **3** with 50% thermal ellipsoids and labeling schemes. All hydrogen atoms are omitted for clarity.

perpendicular to the bromobenzene plane. The shortest intermolecular Pt−Pt separation distance in **3** is 4.873(6) Å. The molecules of **3** form a $\pi-\pi$ stacked dimer structure via their 2-(2′-pyridyl)benzimidazolyl units (see Supporting Information) with the distance between the stacked planes being 3.50 Å.

The common and important feature observed for the structures of **1**−**3** is that the coordination plane of the Pt center (or the plane of the 2-(2′-pyridyl)benzimidazolyl group) is nearly perpendicular to the benzene ring that is attached to the 2-(2′-pyridyl)benzimidazolyl group. We believe that this is caused by the steric interaction between the *ortho* hydrogen atom (i.e. H(16) in **1** and **2**) of the pyridyl ring and the hydrogen atoms of the central benzene ring (for **1**) or biphenyl rings (for **2**). For the free ligands, this interaction can be readily avoided by the free rotation of the pyridyl ring to bring the *ortho* hydrogen away from the central benzene or biphenyl rings. For the complexes, however, the pyridyl can no longer rotate freely due to its

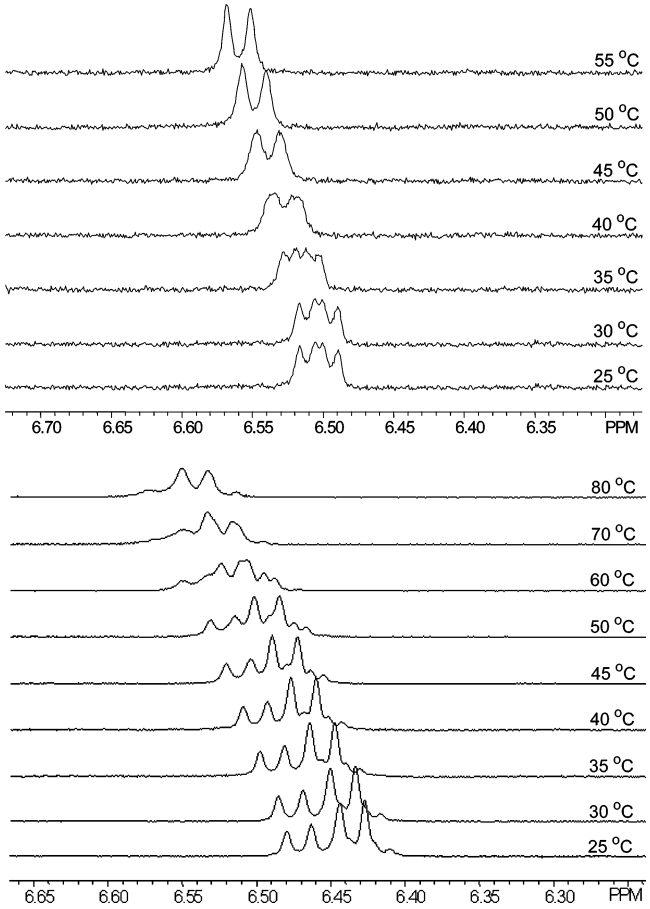

Figure 7. Variable-temperature ^{1}H NMR spectra of complexes **1** (top) and **5** (bottom) in DMSO-d_6 showing the change of one of the proton signals on the 2-(2′-pyridyl)benzimidazolyl group.

binding to the Pt center, which is believed to be responsible for the distinct solution behavior of the complexes.

Structures and Fluxionality of Pt^{II} Complexes in Solution. The crystal structure of **1** has an inversion center. Therefore, if **1** retains the same structure in solution, one would expect to see only one set of chemical shifts due to the 2-(2′-pyridyl)benzimidazolyl group. However, surprisingly, as shown in Figure 7, top, two distinct sets of well-resolved peaks in ∼1:1 ratio, corresponding to two different groups of 2-(2′-pyridyl)benzimidazolyl, were observed in the ^{1}H NMR spectrum of **1** in DMSO-d_6 at 25 °C. As the temperature is increased, the peaks become broad. At 40 °C, the two sets of chemical shifts merge into one set. This temperature-dependent spectral change is clearly caused by some dynamic exchange process of **1** in solution. Although the crystal structure of **1** is centrosymmetric (i.e. with the two 2-(2′-pyridyl)benzimidazolyl units on the opposite side of the central benzene ring, shown as the anti structure in Chart 1), a second structural isomer with a C_2 symmetry where both 2-(2′-pyridyl)benzimidazolyl groups are on the same side of the benzene ring (shown as the syn structure in Chart 1) is also possible for **1**. The 2-(2′-pyridyl)-benzimidazolyl units in either the anti or the syn structure are chemically equivalent. Therefore, one distinct set of chemical shift is expected for each of the isomers. The observed two sets of chemical shifts of the 2-(2′-pyridyl)-

Chart 1

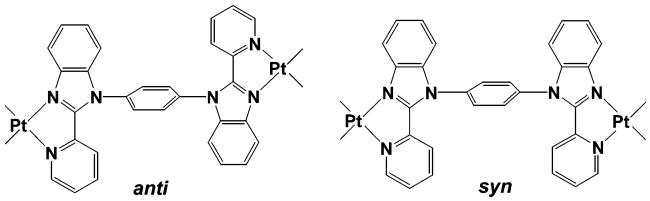

benzimidazolyl groups of **1** at ambient temperature can be attributed to the coexistence of the anti and syn isomers in solution. We believe that both isomers are also likely present in the solid state. The anti isomer is likely to form single crystals more readily than the syn isomer, hence making it possible to identify the anti structure by X-ray diffraction. The fact that both isomers are observed in solution at ambient temperature indicates that the energy barrier for the interconversion of the two isomers must be fairly large. Indeed, with the variable-temperature ^{1}H NMR spectral data, we have estimated that the activation energy for the exchange process of anti and syn structures to be ∼69 kJ/mol by using a previous established method.[16] This large energy barrier is clearly attributable to the hindered rotation of the 2-(2′-pyridyl)benzimidazolyl group with respect to the central benzene ring, due to the *ortho* hydrogen steric interaction and the chelation of the 2-(2′-pyridyl)benzimidazolyl to the Pt atom.

Although the crystal structure of **2** is similar to that of **1**, no dynamic exchange phenomenon was observed for **2** in solution. This is not surprising since the presence of the central biphenyl unit in **2** allows the free rotation around the C−C bond of the biphenyl, thus a facile interconversion of the syn and anti isomers.

Complex **4** where the two 2-(2′-pyridyl)benzimidazolyl groups at 1,3 positions are chelated by two Pt^{II} centers displays a dynamic exchange phenomenon in solution, similar to that of **1**. Again, on the basis of NMR data, both syn and anti isomers of **4** coexist in solution at ambient temperature, which undergo a slow interconversion. The activation energy for the interconversion process was estimated to be ∼65 kJ/mol.

Complex **5** is a very crowded molecule with three 2-(2′-pyridyl)benzimidazolyl groups at 1,3,5 positions chelated to three Pt^{II} centers. Free rotation of the 2-(2′-pyridyl)benzimidazolyl groups with respect to the central benzene ring is therefore unlikely, on the basis of the same arguments for **1** and **4**. On the basis of the arrangement of three 2-(2′-pyridyl)-benzimidazolyl groups, there are two possible structures of **5** in solution, **A** and **B** as depicted in Chart 2. In structure **A**, all of the PtC_2N_2 planes are oriented to the same side of the central phenyl ring with an approximate C_3 symmetry, hence resulting in only one set of chemical shifts of the 2-(2′-pyridyl)benzimidazolyl groups in the NMR spectra. In structure **B**, one of the 2-(2′-pyridyl)benzimidazolyl groups (or the PtC_2N_2 planes) is oriented in the opposite direction from the other two, forming an "two-down−one-up" struc-

(16) Williams, D. H.; Fleming, I. *Spectroscopic Methods in Organic Chemistry*, 4th ed.; McGraw-Hill Co. Ltd.: London, 1987; Chapter 3.

Chart 2

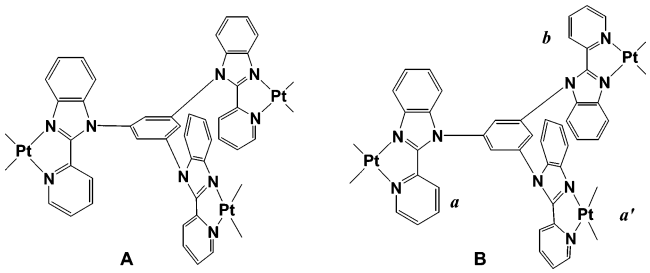

Table 3. Electrochemical Data ($E_{1/2}$ Values for Reductions and Irreversible Oxidation Waves) for Complexes **1**−**5**

compd	E_{ox} (V)	E_{red} (V)	compd	E_{ox} (V)	E_{red} (V)
1[b]	1.16, 1.30	−1.33	**4**[b]	1.18	−1.34
2[b]	1.11	−1.36	**5**[b]	1.15	−1.30
3[a]	0.98	−1.46			

[a] In CH_3CN solution containing 0.10 M (TBA)PF_6 at 293 K, $E_{1/2}$ for $FeCp_2^+/FeCp_2$ (versus AgCl/Ag) = 0.45 V. [b] In DMF solution containing 0.10 M (TBA)PF_6 at 293 K, $E_{1/2}$ for $FeCp_2^+/FeCp_2$ (versus AgCl/Ag) = 0.45 V.

ture, similar to the crystal structure of the free ligand tmb. Because of the presence of an approximate mirror plane symmetry in **B**, relating units *a* and *a*′, two sets of chemical shifts of the 2-(2′-pyridyl)benzimidazolyl groups with a 2:1 ratio should be observed in the ^{1}H NMR spectra. ^{1}H NMR experiments revealed that the molecule of complex **5** adopts mainly the structure **B** in solution at ambient temperature. As shown in Figure 7, bottom, at ambient temperature, well-resolved peaks corresponding to two sets of 2-(2′-pyridyl)-benzimidazolyl groups in 2:1 ratio are observed. The weak peaks could be attributed to the presence of a small amount of structure **A**. As the temperature increases, the spectrum gradually becomes broad. At 80 °C, all peaks start to merge into one set, which can be attributed to the interconversion of the 2-(2′-pyridyl)benzimidazolyl groups of *a* and *a*′ types with that of *b* and the interconversion of the major isomer **B** with the minor isomer **A**. The activation energy for the exchange process of **5** was estimated to be >70 kJ/mol.

Electrochemistry. Cyclic voltammograms recorded for the complexes **1**−**5** in either DMF or CH_3CN all display one reversible reduction wave between −1.20 and −1.50 V (Table 3). On the basis of the previous studies by Kaim and others[17] on Pt(diimine)R_2 and by Eisenberg[18] on Pt(diimine)-$(C{\equiv}CR)_2$ where similar reversible reduction waves were observed and attributed to one electron reduction of the diimine ligand, we assigned the reversible reduction wave to one-electron reduction of the benzimidazolyl chelate ligand in the complexes. The reduction potential shows considerable variation for the five complexes. Since the $PtPh_2$ portion is the same for all complexes, this variation can be only attributed to the variation of the chelate ligand. Complexes

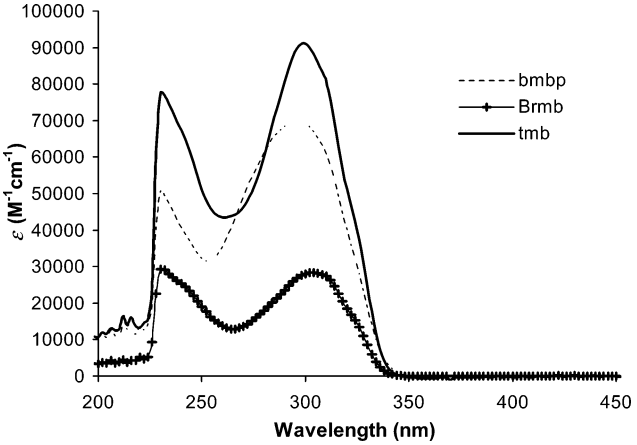

Figure 8. UV−vis absorption spectra of bmbp, Brmb, and tmb in CH_2Cl_2. The absorption spectra of 1,4-bmb and 1,3-bmb are similar to that of bmbp.

Table 4. UV−Vis Absorption Data for the Ligands and the Complexes

compd	abs (nm) (ϵ, $M^{-1}\,cm^{-1}$) in CH_2Cl_2, 298 K[a]
1,4-bmb	230 (63 000), 300 (73 000)
bmbp	230 (51 000), 296 (70 000)
Brmb	232 (29 000), 302 (28 000)
1,3-bmb	232 (65 000), 306 (79 000)
tmb	230 (78 000), 300 (91 000)
1	234 (66 000), 324 (37 000), 456 (6400)
2	240 (73 000), 322 (42 000), 444 (6300)
3	234 (38 000), 322 (18 000), 440 (2900)
4	234 (73 000), 322 (42 000), 458 (6600)
5	234 (94 000), 324 (50 000), 478 (9100)

[a] [M] = 4.8×10^{-6}−2.9×10^{-5} M in CH_2Cl_2.

1 and **4** with the 1,4- and 1,3-disubstituted ligands, 1,4-bmb and 1,3-bmb, respectively, display similar reduction potential (−1.33 and −1.34 V) while complex **2** with the disubstituted biphenyl ligand bmbp has a more negative reduction potential (−1.36 V). Complex **5** with the trisubstituted ligand tmb has the most positive reduction potential (−1.30 V). For the benzene derivative ligands, the data indicate that as the number of 2-pyridylbenzimidazolyl units increase in the ligand, it becomes easier to reduce the complex.

All complexes display an irreversible oxidation wave. For complexes that contain the benzene derivative ligands (**1**, **4**, **5**), the variation of this oxidation potential is very small. On the basis of the previous reports on related diimine Pt(II) complexes,[17] we assigned this oxidation wave to the oxidation of the Pt(II) center.

Absorption Spectra. The absorption spectra of the free ligands 1,4-bmb, bmbp, Brmb, 1,3-bmb, and tmb are similar (Figure 8). Two absorption bands with $\lambda_{max} \approx 230$ and 300 nm were observed for all free ligands, which are attributed to the $\pi \rightarrow \pi^*$ transition centered on the 2-(2′-pyridyl)-benzimidazolyl units. This is supported by the extinction coefficients of the absorption bands. As shown in Table 4 and Figure 8, the ϵ values of 1,4-bmb, bmbp, and 1,3-bmb are approximately twice of that of Brmb and tmb has a ϵ value about three times of that of Brmb. Clearly the ϵ value is linearly dependent on the number of 2-(2′-pyridyl)-benzimidazolyl units present in the molecule. For the benzene derivative ligands 1,4-bmb, 1,3-bmb, Br-bmb, and tmb, the

(17) Klein, A.; Kaim, W. *Organometallics* **1995**, *14*, 1176 and references therein.
(18) (a) Hissler, M.; Connick, W. B.; Geiger, D. K.; McGarrah, J. E.; Lipa, D.; Lachicotte, R. J.; Eisenberg, R. *Inorg. Chem.* **2000**, *39*, 447. (b) Paw, W.; Cummings, S. D.; Mansour, M. A.; Connick, W. B.; Gieger, D. K.; Eisenberg, R. *Coord. Chem. Rev.* **1998**, *171*, 125. (c) McGarrah, J. E.; Kim, Y. J.; Hissler, M.; Eisenberg, R. *Inorg. Chem.* **2001**, *40*, 4510.

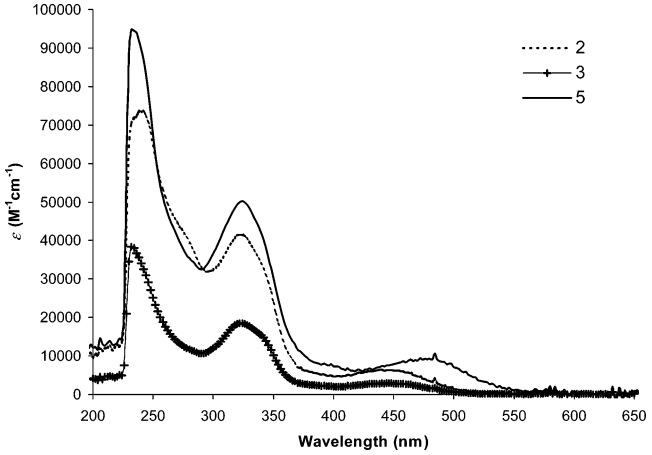

Figure 9. UV−vis absorption spectra of complexes **2**, **3**, and **5** in CH_2Cl_2. The absorption spectra of complexes **1** and **4** are similar to that of **2**.

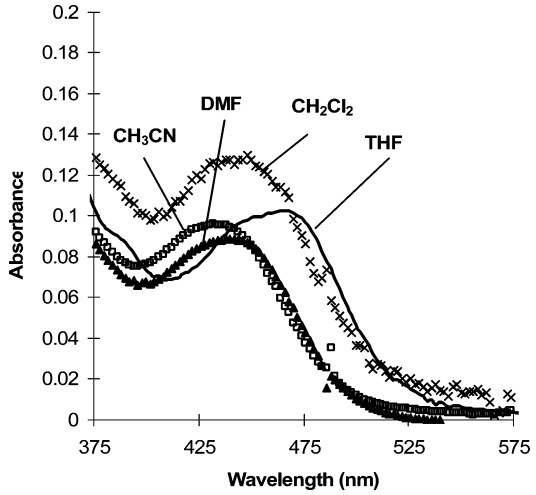

Figure 10. Low-energy region of the UV−vis absorption spectra of complex **2** in various solvents.

absorption band at ∼300 nm shows a small shift toward the longer wavelength as the number of substituent groups increases.

The absorption spectra of complexes **1**−**5** have similar features (Figure 9). Besides the intense absorption bands in UV region ($\lambda_{max} \approx 232$ and 322 nm), which are assigned to the ligand-centered $\pi \rightarrow \pi^*$ transition, all of the complexes have a broad and weak absorption band that covers the region of 410−550 nm ($\lambda_{max} = 445-480$ nm), resulting in the orange-red appearance of complexes **1**−**5**. These absorption bands display the typical negative solvatochromism, i.e., a high-energy shift in a more polar solvent, as demonstrated by the absorption spectra of complex **2** in various solvents (Figure 10), which is consistent with the assignment of MLCT transitions ($d_{Pt} \rightarrow \pi^*$) involving the Pt center and the 2-(2′-pyridyl)benzimidazolyl unit.[17,18] Again, the ϵ values of the absorption bands for complexes **1**−**5** show a linear dependence on the number of 2-(2′-pyridyl)benzimidazolyl units present in the molecule. For example, the ϵ values of the MLCT bands for complexes **1**, **2**, and **4** are approximately twice of that of **3** and **5** has a ϵ value about three times of that of **3**. The absorption maxima of the MLCT bands shift to lower energy as the number of 2-(2′-pyridyl)benzimidazolyl units increases in the complex, an indication of the

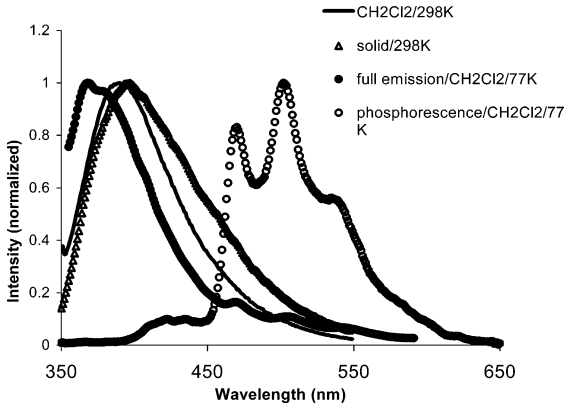

Figure 11. Emission spectra of tmp. (The phosphorescent emission spectrum was obtained using a time-resolved phosphorescence spectrometer.)

presence of some degree of communication among the 2-(2′-pyridyl)benzimidazolyl units. On the basis of the electrochemical data, this low energy shift can be attributed mostly to the decrease of the LUMO energy level associated with the increase of the number of 2-(2′-pyridyl)benzimidazolyl units.

Luminescent Properties. At ambient temperature, all free ligands have purple/blue emission with $\lambda_{max} \approx 365-415$ nm in CH_2Cl_2 solution, which are assigned to fluorescent emissions originating from a ligand-centered $\pi \rightarrow \pi^*$ transition. In the solid state, the fluorescent emissions of the free ligands are red-shifted to 386−431 nm, which is attributable to intermolecular interactions—most likely $\pi-\pi$ stacking interactions, as seen in the crystal structures. No phosphorescent emission bands were observed for the free ligands at ambient temperature. However, at 77 K, in addition to the intense fluorescent bands, new low-energy emission bands ($\lambda_{max} = \sim 500$ nm) with well-resolved vibrational intervals ($\sim 1300-1400$ cm^{-1}) were observed for all ligands. Using a time-resolved phosphorescence spectrometer, we were able to completely remove the fluorescent emission bands and determine the decay lifetimes of these low energy emission bands to be in the range of 7.0(1)−13.2(6) μs, indicating phosphorescent emission. The phosphorescent emission spectrum and the full emission spectrum of tmb are shown in Figure 11 as a representative example. The complete luminescent data are given in Table 5. The full emission and phosphorescent spectra of 1,4-bmb, bmbp, Brmb, and 1,3-bmb are provided in the Supporting Information.

The Pt^{II} complexes **1**−**5** do not display any detectable emission in solution at ambient temperature. At 77 K, the frozen solution (CH_2Cl_2, THF, or CH_3CN) of complexes **1**−**5** exhibit an intense emission band with λ_{max} at ∼537−601 nm (Table 5). The emission spectra of complex **5** along with the free ligand's phosphorescent emission spectrum are shown in Figure 12 to illustrate the impact of the Pt(II) coordination. The emission spectra of complexes **1**−**4** are provided in the Supporting Information. No significant shift of the emission maxima was observed when different solvents were used. The lack of emission of the Pt(II) complexes in solution at ambient temperature is most likely caused by the thermal quenching of the solvent molecules.

Table 5. Luminescence Data for the Ligands and the Complexes

compd	excitatn wavelength, nm	emission bands λ_{max}, nm[a]	decay lifetime τ, μs	conditns
1,4-bmb	331	365		CH_2Cl_2/298 K
	336	386		solid/298 K
	335	379, 470, 505, 542 (sh)[b]		CH_2Cl_2/77 K
	335	469, 502, 534 (sh)	9.2(5), 8.4(3)	CH_2Cl_2/77 K[c]
bmbp	343	415		CH_2Cl_2/298 K
	373	426		solid/298 K
	335	388, 471, 503, 543 (sh)		CH_2Cl_2/77 K
	335	467, 499, 534 (sh)	13.2(6), 10.0(3)	CH_2Cl_2/77 K[c]
Brmb	332	373		CH_2Cl_2/298 K
	344	400		solid/298 K
	334	370, 471, 505, 543 (sh)		CH_2Cl_2/77 K
	334	469, 501, 535 (sh)	8.9(5), 8.7(3)	CH_2Cl_2/77 K[c]
1,3-bmb	334	365		CH_2Cl_2/298 K
	340	431		solid/298 K
	335	370, 470, 500, 540 (sh)		CH_2Cl_2/77 K
	335	466, 498, 534 (sh)	7.2(1), 7.0(1)	CH_2Cl_2/77 K[c]
tmb	338	390		CH_2Cl_2/298 K
	330	397		solid/298 K
	335	371, 472, 509, 543 (sh)		CH_2Cl_2/77 K
	335	470, 503, 539	8.2(3), 7.5(2)	CH_2Cl_2/77 K[c]
1	466	582	7.9(4)	solid/298 K
	424	537, 575 (sh)	7.5(2), 6.8(3)	CH_2Cl_2/77 K
2	466	587	8.0(3)	solid/298 K
	420	552, 583 (sh)	7.8(3), 7.0(2)	CH_2Cl_2/77 K
3	466	592	7.5(2)	solid/298 K
	420	550, 584 (sh)	7.1(2), 6.5(1)	CH_2Cl_2/77 K
4	465	611	8.1(4)	solid/298 K
	432	560, 600 (sh)	7.9(4), 7.2(2)	CH_2Cl_2/77 K
5	466	621	8.2(2)	solid/298 K
	409	601, 631 (sh)	8.4(2), 7.6(3)	CH_2Cl_2/77 K

[a] [M] = 5.9×10^{-5}–3.4×10^{-5} M. [b] sh = shoulder. [c] Obtained using a time-resolved phosphorescence spectrometer.

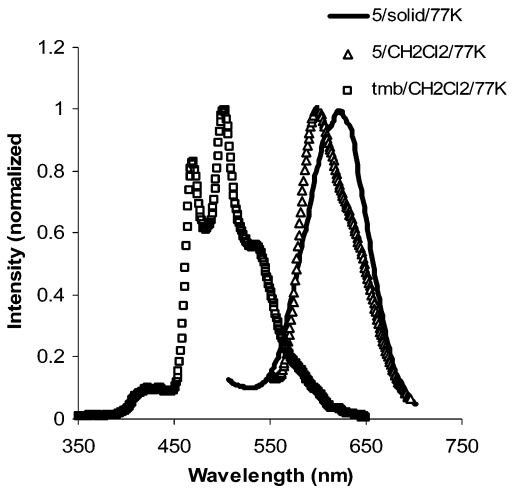

Figure 12. Emission spectra of complex **5** and the phosphorescent spectrum of the tmb ligand at 77 K.

As shown by the data in Table 5 and Figure 12, the phosphorescent emission band of the free ligand is at a much higher energy than that of the corresponding Pt^{II} complex, an indication that the emission of the complex is likely not a ligand-based transition. Furthermore, the emission energy of the complexes (**1**, **2**, **4**, and **5**) changes in the same manner as the MLCT absorption band does, i.e., shifting to lower energy as the number of 2-(2′-pyridyl)benzimidazolyl units increases in the complex. By taking into consideration of the absorption data and the electrochemical data, we suggest that the emission of the complexes at 77 K originates most likely from a MLCT excited state. The solids of all the Pt^{II} complexes display orange-red emission with $\lambda_{max} \approx 582$–621 nm at ambient temperature. The energy of these emissions is independent of excitation wavelength and is somewhat red-shifted from the corresponding emission band of the frozen solutions, likely a consequence of intermolecular interactions in the solid state. The decay lifetime of the emission bands of complexes **1**−**5** were determined to range from 6.5(1) to 8.4(2) μs (Table 5).

Conclusions. The syntheses of five new luminescent organic molecules based on the 2-(2′-pyridyl)benzimidazolyl chromophore have been achieved. These new ligands have been found to bind to the Pt^{II} center readily via N,N-chelation to form the corresponding mononuclear, dinuclear, and trinuclear Pt^{II} complexes. X-ray crystal structural data indicate that the 2-(2′-pyridyl)benzimidazolyl unit has little conjugation with the benzene or the biphenyl groups to which it is directly attached to. Instead, this unit is usually perpendicular to the benzene or the biphenyl group to minimize steric interaction between *ortho* hydrogen atoms. As a consequence of the different orientation of the 2-(2′-pyridyl)benzimidazolyl units with the respect to the central benzene ring and the restricted rotation, structural isomers for complexes **1**, **4**, and **5** were observed in solution. For the free ligands, because the *ortho* hydrogen interactions can be minimized by the free rotation of the pyridyl group, no structural isomers were observed in solution. The emission of the free ligands at ambient temperature and at 77 K is dominated by fluorescence while the emission of the Pt^{II} complexes involves phosphorescence only. The orange-red phosphorescent emission of the Pt^{II} complexes has been found to be most likely MLCT transitions involving the Pt^{II} center and the 2-(2′-pyridyl)benzimidazolyl chelate. Although the Pt(II) complexes do not emit in solution at ambient

temperature, they do emit in the solids at ambient temperature, which renders them potentially useful as phosphorescent emitters for OLEDs.

Acknowledgment. We thank the Natural Sciences and Engineering Research Council for financial support.

Supporting Information Available: Complete listing of crystal data for the free ligands and complexes **1**−**3**, including lattice packing diagrams, crystallographic data in CIF format, complete excitation and emission spectra, variable-temperature ^{1}H NMR spectra for **1** and **4**, and tables of atomic coordinates, thermal parameters, bond lengths and angles, and hydrogen parameters. This material is available free of charge via the Internet at http://pubs.acs.org.

IC0487530